

Prostate-specific membrane antigen associates with anaphase-promoting complex and induces chromosomal instability

Sigrid A. Rajasekaran,¹ Jason J. Christiansen,²
Ingrid Schmid,³ Eri Oshima,²
Kathleen Sakamoto,^{2,3} Jasminder Weinstein,⁴
Nagesh P. Rao,² and Ayyappan K. Rajasekaran¹

¹Nemours Center for Childhood Cancer Research, Alfred I. DuPont Hospital for Children, Wilmington, Delaware; Departments of ²Pathology and Laboratory Medicine and ³Hematology/Oncology, David Geffen School of Medicine, University of California-Los Angeles, Los Angeles, California; and ⁴Amgen, Inc., Thousand Oaks, California

Abstract

Prostate-specific membrane antigen (PSMA) is a transmembrane protein highly expressed in advanced and metastatic prostate cancers. The pathologic consequence of elevated PSMA expression is not known. Here, we report that PSMA is localized to a membrane compartment in the vicinity of mitotic spindle poles and associates with the anaphase-promoting complex (APC). PSMA-expressing cells prematurely degrade cyclin B and exit mitosis due to increased APC activity and incomplete inactivation of APC by the spindle assembly checkpoint. Further, expression of PSMA in a karyotypically stable cell line induces aneuploidy. Thus, these findings provide the first evidence that PSMA has a causal role in the induction of aneuploidy and might play an etiologic role in the progression of prostate cancer. [Mol Cancer Ther 2008;7(7):2142–51]

Introduction

Prostate-specific membrane antigen (PSMA) is localized to secretory cells within the prostatic epithelium and is up-regulated in advanced prostate carcinoma and metastatic disease (1). PSMA is a type II transmembrane protein with a short, NH₂-terminal cytoplasmic tail, a single transmembrane domain, and a large extracellular COOH-terminal

domain and exhibits both *N*-acetylated α -linked acidic peptidase (NAALADase) and folate hydrolase activities (1, 2). Although the physiologic and pathologic functions of PSMA remain unclear, it is of particular interest that PSMA expression is a universal feature of prostate carcinoma. PSMA expression increases with tumor aggressiveness, with greatest levels being found in high-grade tumors, metastatic lesions, and androgen-independent disease (3). This salient association between PSMA expression levels and tumor stage alludes to a potential etiologic role for PSMA in the pathogenesis and progression of prostate cancer.

Progression through mitosis relies on a complex series of precisely coordinated events that is primarily regulated by the periodic rise and fall of mitotic B-type cyclin levels. During the late stages of G₂, elevated levels of the mitotic B-type cyclins permit cellular alterations associated with mitosis, such as nuclear envelope breakdown and chromosome condensation. As these cells enter into mitosis, the newly replicated centrosomes migrate to opposing ends of the cell to serve as the mitotic spindle poles. The spindle poles nucleate a dense array of microtubules that attach in a bipolar manner to the kinetochores on the condensed chromosomes (4, 5). As the condensed chromosomes attach to spindle microtubules and become properly aligned at the metaphase plate, a large multisubunit ubiquitin ligase known as the anaphase-promoting complex (APC) becomes activated and degrades cyclin B (5, 6). The degradation of cyclin B allows the cells to exit mitosis and enter a subsequent round of the cell cycle (7).

Although the principle function of spindle poles was believed previously to be limited to nucleation of microtubules, more recent evidence alludes to additional roles in signal transduction and cell cycle regulation. It is now evident that centrosomes play a crucial role in the timing of mitotic events, such as the cyclin B degradation in early *Drosophila* embryos and exit of cytokinesis in animal cells (8, 9). Immunofluorescence analysis has also showed that APC accumulates at the centrosomes and that the spindle poles are where the ubiquitination of cyclin B is initiated (10). Furthermore, several proteins involved in spindle assembly checkpoint function and temporal regulation of mitosis have also been localized to the centrosomes and spindle poles, including Mad2, Bub2, and Bfa1 (11–14).

The activity of APC is highly regulated by checkpoint mechanisms that prevent APC activation and entry into anaphase (15, 16). Several mutations and epigenetic defects affecting mitotic checkpoint components, including RASSF1A, Bub1, BubR1, Mad2, and Mad1, have all been identified in various forms of solid and hematologic malignancies (17–22). Premature activation of APC would

Received 1/4/08; revised 3/6/08; accepted 3/8/08.

Grant support: Department of Defense grant W81XWH-04-1-0113 and NIH grant DK56216.

The costs of publication of this article were defrayed in part by the payment of page charges. This article must therefore be hereby marked *advertisement* in accordance with 18 U.S.C. Section 1734 solely to indicate this fact.

Note: S.A. Rajasekaran and J.J. Christiansen contributed equally to this work.

Requests for reprints: Ayyappan K. Rajasekaran, Nemours Center for Childhood Cancer Research, Alfred I. DuPont Hospital for Children, Rockland Center I, 1701 Rockland Road, Wilmington, DE 19803. Phone: 302-651-6593; Fax: 302-651-4827. E-mail: araj@medsci.udel.edu
Copyright © 2008 American Association for Cancer Research.
doi:10.1158/1535-7163.MCT-08-0005

provide less time for proper chromosome attachment and alignment and would thus reduce the fidelity of chromosomal segregation into daughter cells. This type of chromosomal instability is by far the most frequent form of genetic instability among solid tumor cells and manifests in gross gains or losses of one or more chromosomes, a condition known as aneuploidy. Aneuploidy is apparent during the earliest stages of malignant transformation, has been implicated as a driving force in the process of tumorigenesis (17–19, 21, 22), and may have a central etiologic role in inducing the complex phenotypes associated with cancer by altering the expression and balance of literally thousands of structural and regulatory genes.

In this study, we show that PSMA, a membrane protein, is localized to a membrane compartment in the vicinity of centrosomes at the spindle poles and associates with APC leading to premature activation of APC and induction of aneuploidy. These studies suggest that PSMA has a causal role in the progression of prostate cancer.

Materials and Methods

Cell Lines and Immunofluorescence

PC3 cells expressing PSMA (PC3-PSMA) (23, 24) and Madin-Darby canine kidney (MDCK) cells expressing PSMA (MDCK-PSMA) or a deletion construct lacking amino acids 103 to 750 of the extracellular domain of PSMA (MDCK-PSMA- Δ 103-750; refs. 25, 26) were described previously. A cytoplasmic tail deletion construct of PSMA (PSMA- Δ CD; ref. 27) was stably expressed in MDCK cells (25). For HCT-116 cells expressing PSMA (HCT-PSMA), PSMA was cloned from LNCaP cells and lentivirus harboring PSMA was transduced. HCT-116 cells expressing GFP (HCT-GFP) were generated as control.

Immunofluorescence analysis was done as described (25, 27) using monoclonal antibody J591 against the extracellular domain of PSMA (28) and rabbit anti-pericentrin (Covance Research Products). 4',6-Diamidino-2-phenylindole was used to visualize nuclei and chromosomes. Micrographs were taken with an Axiophot microscope (Zeiss) equipped with a triple filter (4',6-diamidino-2-phenylindole/FITC/Texas red).

Cell Synchronization and Cell Cycle Analysis

A G₂-M block was induced with 100 nmol/L nocodazole for 10 h and mitotic cells were harvested by trypsinization and gentle tapping of the culture dish. The mitotic block was released, and at each indicated time point, cells were harvested and fixed in 70% ethanol. DNA was stained with 100 μ g/mL propidium iodide and 20 μ g/mL RNase A in hypotonic citrate buffer. Samples were analyzed on a FACSCalibur flow cytometer (BD Biosciences) as described (29). Analysis of multivariate data was done with CellQuest software (BD Biosciences) and DNA histograms generated with ModFit LT software (Verity Software House).

Immunoblot Analysis and *In vitro* APC Assay

Total protein (100 μ g) from synchronized and mitotic block-released PC3 and PC3-PSMA cells lysed in 95 mmol/L NaCl, 25 mmol/L Tris (pH 7.4), 0.5 mmol/L EDTA, 2% SDS,

1 mmol/L phenylmethylsulfonyl fluoride, and 5 μ g/mL each of antipain, leupeptin, and pepstatin (protease inhibitor cocktail) were used for immunoblot analysis using anti-cyclin B1 (Santa Cruz Biotechnology). Proteins were detected by enhanced chemiluminescence and quantified by densitometry. Immunoblot analysis of nonsynchronized and G₂-M PC3 and PC3-PSMA cells were done using anti-Mad2, BubR1, Cdc20 (30), and Cdc27 (BD Transduction Laboratories) antibodies.

In vitro APC assays were done using an *in vitro* transcribed and translated NH₂-terminal fragment of cyclin B₁ (cyclin B₁-N₁₋₁₀₂) as substrate. Amino acids 1 to 102 of cyclin B₁ were amplified by PCR and subcloned into pCDNA3. [³⁵S]methionine-labeled cyclin B₁-N₁₋₁₀₂ was obtained using the TNT quick-coupled transcription/translation system (Promega). Cell pellets of synchronized PC3 and PC3-PSMA cells were snap frozen in liquid nitrogen and cell lysates were prepared by incubating for 30 min in an ice-cold hypotonic buffer [20 mmol/L HEPES (pH 7.6), 20 mmol/L NaF, 1.5 mmol/L MgCl₂, 1 mmol/L DTT, 5 mmol/L KCl, 20 mmol/L β -glycerophosphate, 250 μ mol/L NaVO₃, 1 mmol/L phenylmethylsulfonyl fluoride, and EDTA-free protease inhibitors] followed by brief homogenization. Total protein (30 μ g) from cell lysate supernatants (1 h centrifugation at 13,000 rpm at 4°C in a microcentrifuge) was added to reaction buffer containing 20 mmol/L Tris (pH 7.5), 20 mmol/L NaCl, 5 mmol/L MgCl₂, 5 mmol/L ATP- γ -S, 20 μ g/mL MG-132, 0.5 μ g Ubc10, 20 μ mol/L ubiquitin, 1 μ mol/L ubiquitin aldehyde, protease inhibitors, and 2 μ L *in vitro* translated [³⁵S]methionine cyclin B₁-N₁₋₁₀₂. Reactions were incubated at 37°C for 60 min. Samples were separated by SDS-PAGE (4-15% gradient gel), enhanced with salicylate, and subjected to autoradiography.

Coimmunoprecipitation and *In vitro* Binding Assays

Cell lysates of nonsynchronized cells or from PSMA-positive prostate tumor tissue lysates were prepared in 20 mmol/L Tris (pH 7.4), 150 mmol/L NaCl, 1 mmol/L EDTA, 1 mmol/L EGTA, 1% Triton X-100, 1 mmol/L β -glycerophosphate, 1 mmol/L NaVO₃, 2.5 mmol/L sodium pyrophosphate, 50 mmol/L NaF, and protease inhibitor cocktail. Cdc27 was immunoprecipitated using goat anti-Cdc27 (Santa Cruz Biotechnology) and PSMA with monoclonal antibody J591 for 16 h at 4°C. Coimmunoprecipitating proteins were detected by immunoblotting. *In vitro* pull-down assays from PC3 cells were done using a purified GST-PSMA fusion protein as described (24). A monoclonal anti-Cdc27 antibody (BD Transduction Laboratories) was used to detect Cdc27 in both coimmunoprecipitates and GST pull-downs.

Cytogenetics and Fluorescence *In situ* Hybridization

Early passages from HCT cells were analyzed by standard cytogenetics. About 25 metaphases were analyzed and karyotyped to determine chromosome number and structure consistency. Fluorescence *in situ* hybridization was used to determine the aneuploidy in cells obtained from a series of cell passages (2, 15, 34, and 45) of HCT-PSMA and HCT-GFP cells. To establish a generalized

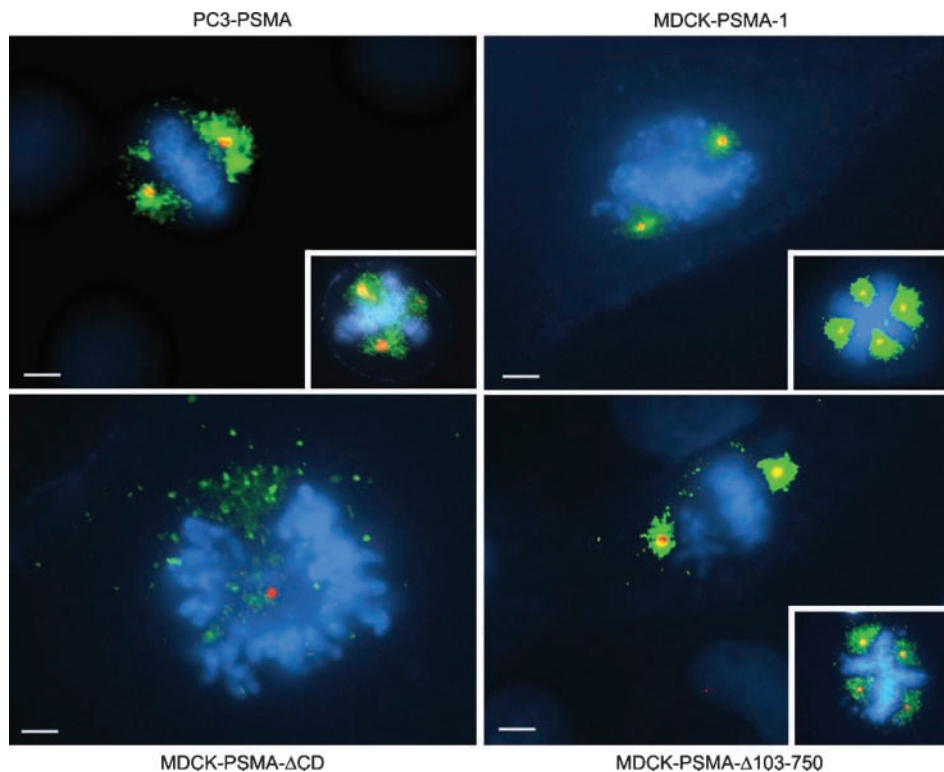


Figure 1. Localization of PSMA at the mitotic spindle poles. Note distinct colocalization of PSMA (green) with centrosomes (red) at the mitotic spindle poles in PC3-PSMA, MDCK-PSMA-1, and MDCK-PSMA- Δ 103-750 cells but not in MDCK-PSMA- Δ CD cells. Bar, 8 μ m.

mechanism of chromosome number variation, fluorescence *in situ* hybridization analyses with DNA probes specific for the centromeres of chromosome 3, 7, 17, and 9p21 region, respectively, were used (Abbott-Vysis). These probes are labeled variously as a cocktail for multicolor fluorescence *in situ* hybridization analysis (Urovysion probe panel). Cells that easily detached were fixed and hybridized with the Urovysion probe panel following the manufacturer's recommendation. Interphase cells with multicolor probe signals were examined under a fluorescent microscope (Axiophot; Zeiss) equipped with appropriate filters. Approximately, 1,000 nuclei were analyzed for each passage and cell type.

Immuno-Electron Microscopy

Cells fixed in ice-cold methanol were incubated with monoclonal antibody J591 as described for immunofluorescence, washed, and then incubated with 10 nm gold-conjugated anti-mouse secondary antibody. After washing, cells were fixed in 2.5% glutaraldehyde in cacodylate buffer and scraped off the plate and cell pellets were processed by conventional electron microscope procedures.

Results

To elucidate whether expression of PSMA itself has a role in prostate cancer progression, full-length protein was expressed in PC3 cells (PC3-PSMA), a prostate cancer cell line devoid of endogenous PSMA (23). In addition to its plasma membrane localization (24), PSMA was distinctly evident in the vicinity of mitotic spindle poles around

centrosomes (Fig. 1). Localization to the mitotic spindle pole regions was also observed in stable clones of MDCK cells expressing PSMA (MDCK-PSMA-1; ref. 25; Fig. 1). Strikingly, cells with multiple centrosomes showed PSMA localized around each additional centrosome in both PC3-PSMA and MDCK-PSMA cells (Fig. 1, *inserts*). Localization to the spindle pole region was contingent on the cytoplasmic tail of PSMA, as removal of this domain (PSMA- Δ CD) resulted in the loss of localization around the centrosomes with expression primarily limited to the plasma membrane (27) and trans-Golgi network (Fig. 1). Furthermore, a PSMA deletion mutant lacking most of its extracellular domain (MDCK-PSMA- Δ 103-750; ref. 26) showed distinct localization in the vicinity of mitotic spindle poles (Fig. 1), indicating that the glutamate carboxyl peptidase activity of PSMA, which is localized to the extracellular domain (1), is not necessary for its spindle pole localization. Immunogold electron microscopy further confirmed localization of PSMA around the centrosomes at the spindle pole region. At higher magnification, a distinct labeling proximal to membranes in the centrosomal region was visible (Fig. 2).

Given the function of spindle poles in cell division, we hypothesized that localization of PSMA in the vicinity of spindle poles is associated with a role in mitosis. Cells were synchronized in mitosis by nocodazole and cell cycle progression after its removal was monitored by flow cytometry (Table 1; Fig. 3). Nocodazole treatment blocked >90% of cells in G₂-M with a DNA content of 4N for both PC3 and MDCK cells, irrespective of PSMA expression,

suggesting efficient synchronization of cells in G₂-M (Fig. 3). PC3-PSMA cells and two independent clones of MDCK-PSMA cells (MDCK-PSMA-1 and MDCK-PSMA-2) exited mitosis in an accelerated manner compared with control cells that do not express PSMA (Fig. 3, PC3 and MDCK-pCDNA3, respectively). Strikingly, MDCK-PSMA-ΔCD cells entered G₁ slower than either MDCK-PSMA clone but with a rate closer to that shown by MDCK-pCDNA3 (empty vector) cells (Fig. 3). The MDCK cells exhibited slower recovery from nocodazole release, necessitating the observation of later time points. Furthermore, MDCK-PSMA-Δ103-750 cells entered G₁ faster than MDCK-pCDNA3 cells and similar to MDCK-PSMA cells (Fig. 3). Taken together, these results showed that the

cytoplasmic tail is essential for PSMA localization to the mitotic spindle pole region and accelerated exit from mitosis.

Entry and exit from mitosis are regulated primarily through control of cyclin-dependent kinase 1 activity via ubiquitin-mediated proteolysis of cyclin B (7, 31). As the chromosomes attach to spindle microtubules and become properly aligned at the metaphase plate, APC becomes activated and targets key substrates, including cyclin B, for degradation (32, 33). The mitotic spindle checkpoint halts the action of APC and acts to restrain cells from entering anaphase (16). We hypothesized that accelerated exit from mitosis of PSMA-expressing cells is due to impaired spindle checkpoint with increased APC activity leading to

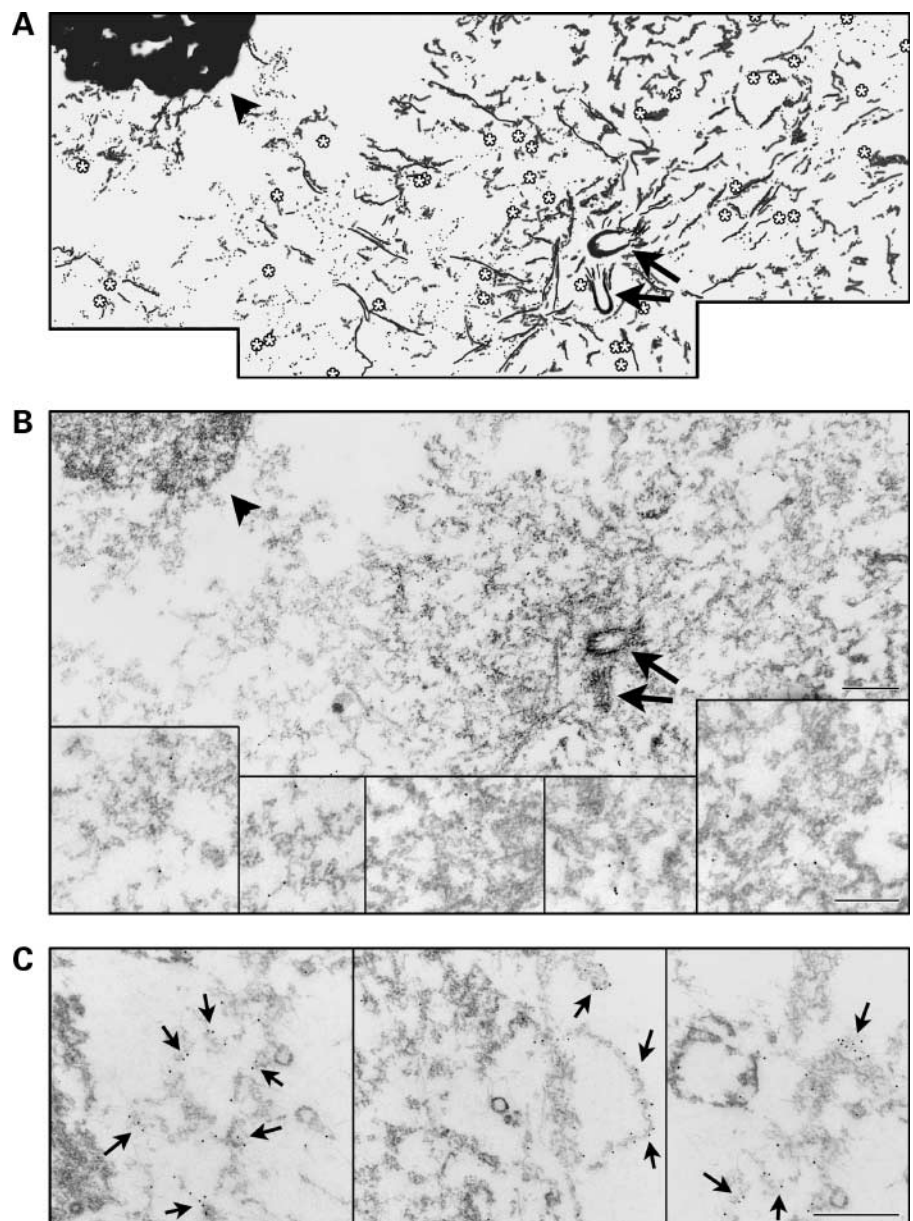


Figure 2. Immunoelectron microscopy showing PSMA localization around the centrosomes. **A**, a cartoon of the electron micrograph shown in **B**. **A** and **B**, arrows, centriolar cylinders; asterisks, gold particles (10 nm) decorating PSMA. One of the spindle poles is shown in this image. Arrowhead, condensed chromatin from metaphase chromosomes in this mitotic cell. **B**, insets, magnified images of regions corresponding to arrows in **B**. **C**, magnification facilitates visualization of gold particles on membrane like structures (arrows). Bar, 0.5 μ m (**A** – **C**).

Table 1. Cell cycle progression in nocodazole-blocked cells

Cell lines	% Cells in G ₁ ± SE after release of nocodazole block		
	60 min	90 min	120 min
PC3	3 ± 1	43 ± 3	69 ± 3
PC3-PSMA	25 ± 2	52 ± 1	79 ± 1
	2 h	4 h	8 h
MDCK-pCDNA3	25 ± 1	29 ± 1	41 ± 2
MDCK-PSMA-1	43 ± 1	53 ± 3	64 ± 1
MDCK-PSMA-2	57 ± 2	64 ± 2	81 ± 3
MDCK-PSMA-ΔCD	25 ± 1	39 ± 1	52 ± 1
MDCK-PSMA-Δ103-750	22 ± 1	43 ± 0	68 ± 3
	1 h	2 h	4 h
HCT-GFP	6 ± 1	22 ± 0	28 ± 2
HCT-PSMA	11 ± 1	43 ± 1	47 ± 3

NOTE: Mean ± SE of two (PC3 and HCT) and three (MDCK) independent experiments.

premature degradation of cyclin B. In PC3-PSMA cells, during nocodazole arrest and following mitotic release, cyclin B1 levels were consistently lower than in control PC3 cells (Fig. 4A), suggesting increased activity and/or incomplete inactivation of the APC in PSMA-expressing cells. To test this possibility, we developed an *in vitro* assay to monitor the ubiquitin ligase activity of APC on cyclin B. Because APC is a large protein complex consisting of >10 subunits and the active enzyme has not been successfully purified *in vitro* (34, 35), we used total cell lysates as the source of APC. Because UbcH10 is the specific ubiquitin-conjugating enzyme (E2) for APC substrates and no other activity has been ascribed to this enzyme, our APC assay specifically detects APC activity. Furthermore, in mitotic HeLa cell lysates, ubiquitination of cyclin B1 was greatly amplified by the addition of increasing amounts of UbcH10 and inhibited by dominant-negative UbcH10.⁵ Relative to PC3 cells, the APC ubiquitin ligase activity for cyclin B was substantially higher at 0, 60, and 120 min after release from nocodazole block in PC3-PSMA cells (Fig. 4B). Therefore, increased APC activity in nocodazole-blocked PC3-PSMA cells indicated that APC is incompletely inactivated by the mitotic spindle checkpoint and confirmed our hypothesis that PSMA expression leads to a weakened spindle assembly checkpoint function in prostate cancer cells.

The APC function is monitored by a complex pattern of regulation (32). Mad2 and BubR1 are well-characterized negative regulators of APC (6), whereas Cdc20 activates APC function (36). However, immunoblot analysis revealed that asynchronous populations of PC3 and PC3-

PSMA cells expressed similar levels of the APC regulators Mad2, BubR1, and Cdc20 and of the core subunit of the APC, Cdc27 (Fig. 5A). The levels of BubR1, Cdc20, and Cdc27 were all increased to a similar extent in mitotically active PC3 cells independent of PSMA expression. Due to phosphorylation, Cdc27 and BubR1 showed multiple bands with the banding pattern and intensity of these bands being comparable in PC3 and PC3-PSMA cells (Fig. 5A). Coimmunoprecipitation analysis using anti-Cdc27 antibody revealed similar levels of Mad2, BubR1, and Cdc20 associated with APC in both PC3 and PC3-PSMA cells (Fig. 5B); in addition, Mad2, BubR1, or Cdc20 was not detected in PSMA immunoprecipitates,⁵ making it unlikely that PSMA activates APC by altering association of these regulators with APC.

We then tested whether PSMA associates with the core APC complex. We observed that in both PC3-PSMA and MDCK-PSMA cells Cdc27 coimmunoprecipitated with PSMA (Fig. 5C, *left*) but not with the cytoplasmic tail deletion mutant of PSMA in MDCK-PSMA-ΔCD cells, confirming that the cytoplasmic tail mediates the association of PSMA with APC. These results were further verified by *in vitro* pull-down assays from PC3-PSMA cell lysates using a GST-fusion protein containing the cytoplasmic tail of PSMA (GST-PSMA-CD; Fig. 5C, *right*). We were also able to coimmunoprecipitate PSMA and Cdc27 in lysates made from six PSMA-positive tumor tissue samples (Fig. 5D). Taken together, these results showed that the cytoplasmic tail of PSMA associates with Cdc27 in both cultured cells and prostate tumor tissues and this association results in an increased APC activity in PSMA-expressing cells.

The elevated APC activity in PSMA-expressing cells resulting in premature degradation of cyclin B1 would provide less time for chromosome segregation, increasing the likelihood of aneuploidy. To assess the significance of

⁵S.A. Rajasekaran et al., unpublished data.

PSMA expression on genomic stability, we expressed PSMA in HCT-116 cells (HCT-PSMA). Derived from colorectal carcinoma, the HCT-116 cell line possesses a nearly diploid karyotype and is an established model for studying chromosomal instability (37). The diploid karyotype of this cell line was confirmed by standard karyotype analysis.⁵ Moreover, because aneuploidy is an irreversible event and because prostate cancer cells expressing PSMA such as LNCaP are aneuploid, RNA interference-mediated knockdown of PSMA in these cells is less likely to provide information as to whether PSMA expression is associated with aneuploidy. Therefore, HCT-116 cells were used as a model to test whether PSMA expression induces aneuploidy. PSMA colocalized with centrosomes in HCT-PSMA cells,⁵ and these cells exited mitosis faster than control HCT-GFP cells (Table 1). Fluorescence *in situ* hybridization was done using probes specific for chromosomes 3, 7, and 17 centromeres and 9p21 region, respectively. No chromosomal abnormalities were observed between HCT-PSMA and HCT-GFP cells at passage 2 (Fig. 6B). However, at higher passage numbers of 15, 34, and 45, all these chromosomes showed various degrees of aneuploidy in HCT-PSMA cells (Fig. 6C-G). The frequency of aneuploidy

increased with passage number, and by passage 45, there was significant increase in the number of aneuploidy in PSMA-expressing cells ($P < 0.001$, $\chi^2 = 13.25$; $n = 1,000$). In addition, clear evidence of micronuclei formation was observed (Fig. 6E, *arrow*, and F), which provided further evidence for chromosomal instability (38).

Discussion

In this study, we report that PSMA is localized to a membrane compartment in the vicinity of the mitotic spindle poles. The J591 monoclonal antibody against PSMA used in this study has been extensively used for immunofluorescence, immunogold labeling, immunoblot, and immunoprecipitation analyses cited in numerous publications (24, 26–28, 39). This antibody detects a single band in immunoblot and immunoprecipitation analysis (25, 28) and cells lacking PSMA expression do not reveal any background staining (27, 39). Therefore, the staining observed around the centrosomes is specific to the localization of PSMA at this site.

Although PSMA is localized to a compartment around the centrosomes, it is important to note that PSMA is not a

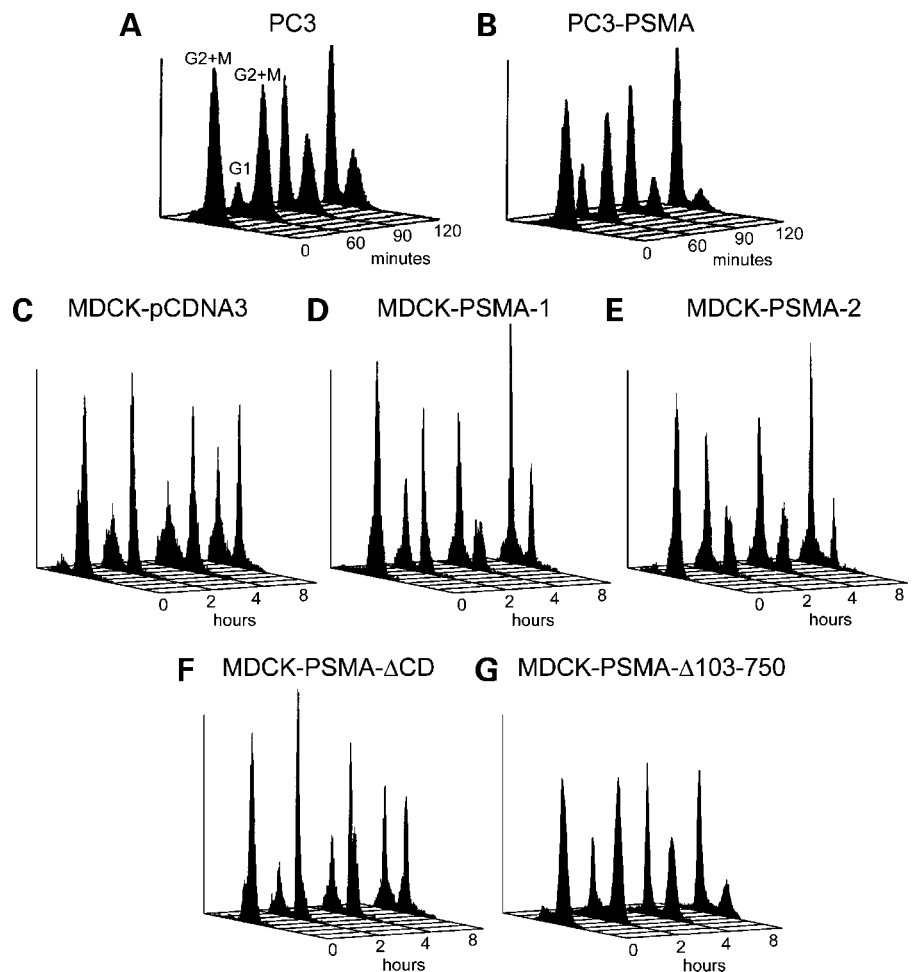


Figure 3. Analysis of the cell cycle progression in PSMA-expressing cells after release of the mitotic block. Cells were blocked in mitosis as described in Materials and Methods. The mitotic block was released for PC3 clones (A and B) and 2, 4, and 8 h for MDCK clones (C–G) and analyzed for cell cycle progression. Representative of the data shown in Table 1.

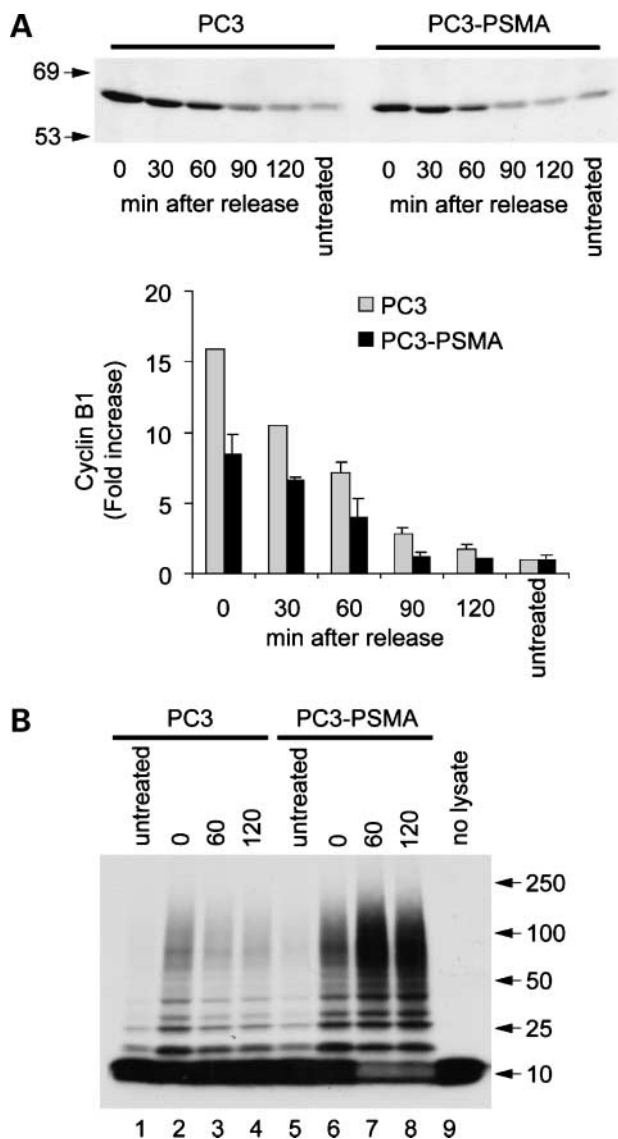


Figure 4. Cyclin B₁ levels and APC activation by PSMA. **A**, immunoblot analysis of cyclin B₁ in PC3 and PC3-PSMA cells after release of the mitotic block. Mean \pm SD of two independent experiments. **B**, *in vitro* APC ubiquitin ligase activity assay in PC3 and PC3-PSMA cells after 60 and 120 min release from nocodazole block.

core centrosomal component. Treatment of cells with nocodazole completely abrogated PSMA localization around the centrosome,⁵ unlike core centrosomal components that still associate with centrosomes following nocodazole treatment. We suggest that PSMA is localized to a membrane compartment around the centrosomes at the vicinity of spindle poles. Recent studies have indicated that important regulators of endocytic traffic, such as clathrin (40, 41), myosin Vb, and rab11 (42), as well as cargo molecules, such as the polymeric IgA receptor (42), are localized to the spindle poles. PSMA is internalized via clathrin-coated pits (28) and expression of K44A dynamin, which inhibits clathrin-dependent endocytosis, prevents

internalization of PSMA (27). These results are consistent with the idea of the presence of a membrane compartment in the vicinity of the spindle poles that is involved in clathrin-mediated endocytosis. At this point, it is not known whether the PSMA localized to the spindle pole is internalized from the plasma membrane or delivered to this site via a biosynthetic route. The origin and nature of this compartment and how PSMA is targeted to this membrane compartment will be addressed in future studies. Interestingly, LNCaP cells that express high levels of endogenous PSMA and which have been widely used as a model in prostate cancer research did not reveal PSMA localization

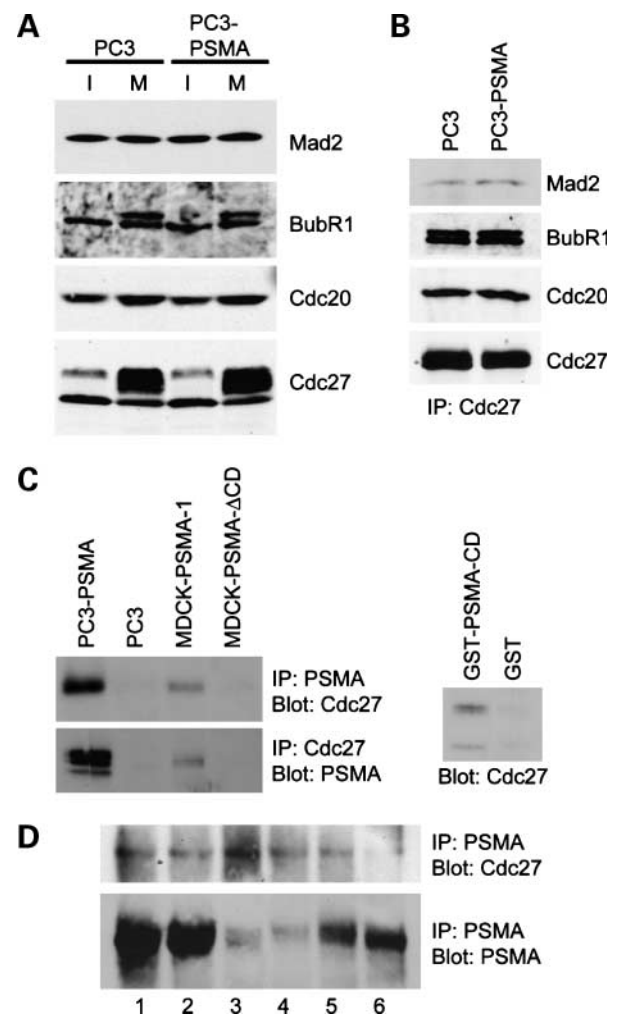


Figure 5. Association of PSMA with APC. **A**, immunoblot analysis of Mad2, BubR1, Cdc20, and Cdc27 in interphase (I) and Mitotic (M) cells. **B**, coimmunoprecipitation of Mad2, BubR1, and Cdc20 with Cdc27 in PC3 and PC3-PSMA cells. Equal amounts of Cdc27 used in the immunoprecipitation was confirmed by immunoblotting. **C**, coimmunoprecipitation of PSMA with Cdc27 (top left) and Cdc27 coimmunoprecipitating PSMA (bottom left) in PC3-PSMA and MDCK-PSMA cells. Note that Cdc27 does not coimmunoprecipitate with PSMA-ΔCD. Affinity precipitation of Cdc27 by GST-PSMA from PC3 cell lysate (right). **D**, coimmunoprecipitation of Cdc27 with PSMA in prostate cancer tissues (top). PSMA levels in same tissues are shown (bottom).

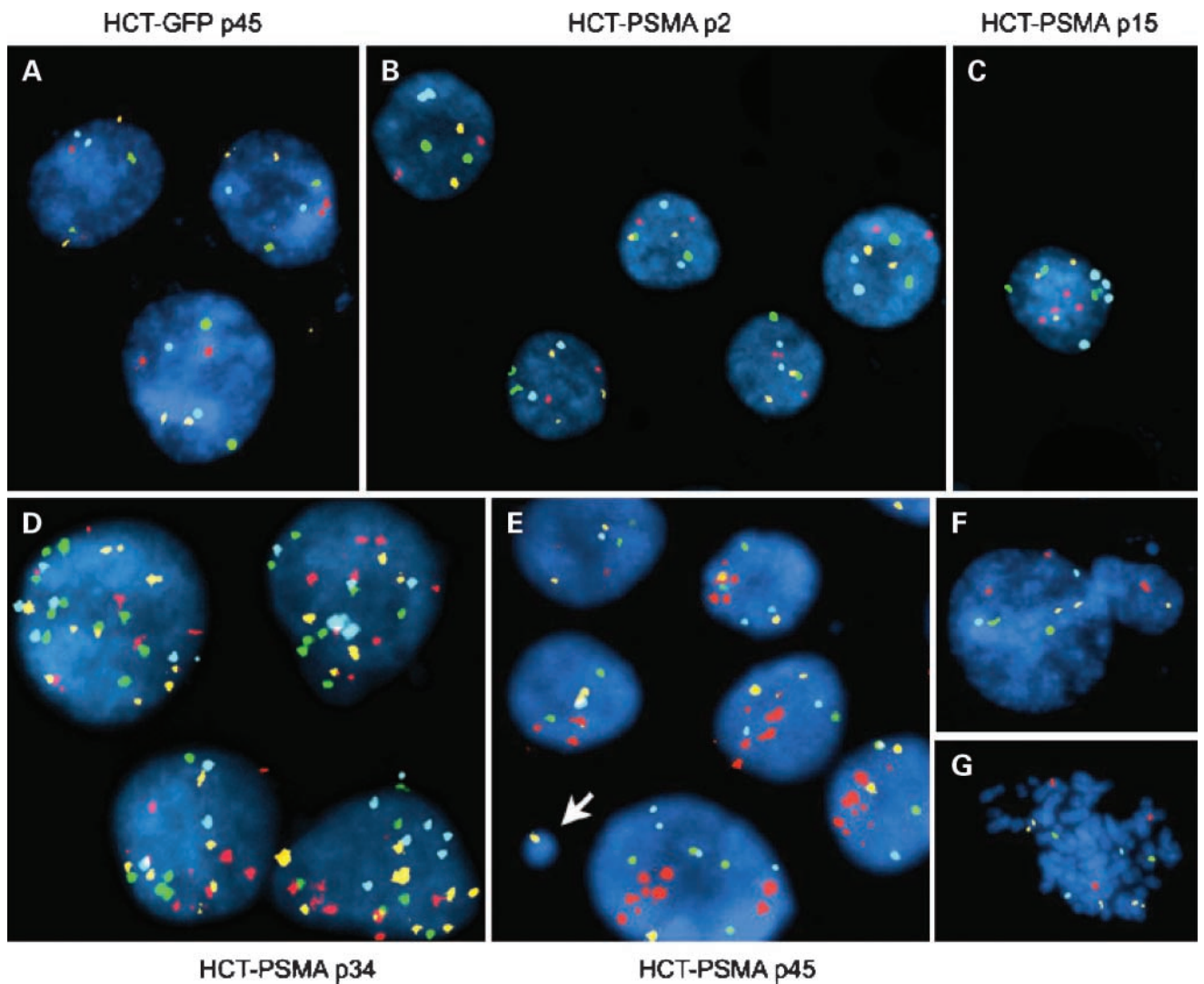


Figure 6. PSMA-expressing human cells are genetically unstable. HCT-PSMA and HCT-GFP cells were analyzed by multicolor fluorescence *in situ* hybridization with chromosome 3 labeled with spectrum red (*CEP3*), chromosome 7 with spectrum green (*CEP7*), chromosome 17 with spectrum aqua (*CEP 17*), and 9p21 region (*p16 gene*) with spectrum gold. Control HCT-GFP cells at passage 45 (**A**) and HCT-PSMA cells at passage 2 (**B**) are diploid, whereas HCT-PSMA cells at passages 15 (**C**), 34 (**D**), and 45 (**E**) show aneuploidy. Micronucleus formation (**E**, arrow, and **F**) and abnormal metaphase (**G**) in HCT-PSMA cells at passage 45 are shown.

around centrosomes. Further analysis in this cell line revealed that this cell line has defects in the organization of key membrane compartments such as Golgi apparatus and endosomes.⁵ Studies are in progress to address the difference in the localization of PSMA in LNCaP cells.

We have shown that PSMA-expressing cells exit mitosis prematurely. Although the effects on cell cycle are small, they are reproducible and significant and have been confirmed in multiple cell lines. Cells expressing the cytoplasmic tail deletion mutant of PSMA progress through the cell cycle similar to control cells without PSMA expression, and PSMA- Δ CD does not associate with APC, establishing further specificity to our experiments. It is important to note that PSMA association with APC

probably does not inhibit the spindle checkpoint per se but rather partially uncouples APC activity either directly or indirectly from spindle checkpoint control. Several reports have described spindle checkpoint proteins such as early mitotic inhibitor (Emi1) and tumor suppressor RASSF1A to inhibit APC by interacting with the activator Cdc20 (22, 36, 43). Recently, the oncoprotein Tax of the human T lymphotropic virus type 1 has been shown to activate APC by directly binding to Cdc20 and leaving the spindle checkpoint intact (44). A protein called Xnf7 is unusual in that it inhibits the APC by interaction with Cdc27 (45). Here, we presented evidence for a protein that mediates APC activation by interaction with Cdc27 and impairing the mitotic spindle checkpoint. This could be

achieved by maintaining high concentrations of the dynamic active APC complex at the spindle poles, a site for initiation of cyclin B1 ubiquitination during mitosis (46). A mechanism for inactivating spindle assembly checkpoint has recently been ascribed to the nondegrading ubiquitination of the mitotic activator subunit Cdc20 by the APC in conjunction with the E2 UbcH10, causing disassociation of checkpoint proteins from Cdc20 (47). Perhaps the increased APC activity observed in the PSMA-expressing cells is sufficient to impair spindle assembly checkpoint activity. Conversely, the deubiquitinating enzyme USP44 deubiquitinates Cdc20 and drives the assembly of the inhibitory spindle assembly checkpoint complexes (48). PSMA could potentially act at any of these steps to increase APC activity. Consequently, the spindle checkpoint would be impaired in performing its function to keep APC inactive. Treatment of cells with strong inhibitors of the spindle checkpoint such as Hesperadin or ZM447439 (Aurora kinase inhibitor) results in these cells entering endoreplication cycles and exhibiting polyploidy within 24 to 48 h. In contrast, in PSMA-expressing cells, aneuploidy is not observed until the 15th passage. The effect is subtle and we believe more relevant to the biological evolution of aneuploidy in a tumor cell.

PSMA is not expressed at high levels in normal prostatic epithelial cells. However, expression is significantly elevated during the progression of cancer, with the greatest levels observed in high-grade tumors, metastatic lesions, and androgen-independent disease. Thus, increased expression of PSMA directly correlates with the aggressiveness of the disease. Low expression of PSMA per se might not constitute a factor leading to aneuploidy, because low levels of PSMA are found in benign prostate tumors and some normal nonprostatic tissues (1, 2). Our data strongly suggest that on increased expression of PSMA the ability of its cytoplasmic tail to associate with the APC complex dysregulates APC function leading to aneuploidy in cancer cells. Thus, PSMA function might not be required for normal cell cycle progression, but its elevated expression and mislocalization at the spindle pole region and association with APC is an accidental and pathologic consequence in cancer cells leading to aneuploidy. An understanding of the putative oncogenic role of PSMA could have major implications for the management and therapy of prostate cancer. Targeted therapies against PSMA-expressing prostate cancer cells are already being evaluated for their potential to treat prostate cancer (49). Because PSMA expression is closely associated with aneuploidy, such anti-PSMA therapeutic strategies might have the advantage of specifically targeting the most aggressive and aneuploid cells.

Disclosure of Potential Conflicts of Interest

No potential conflicts of interest were disclosed.

Acknowledgments

We thank Drs. Warren Heston (Cleveland Clinic Foundation) for PSMA cDNA, Michel Sadelain (Memorial Sloan Kettering Cancer Center) for PC3-

PSMA, Bert Vogelstein (Johns Hopkins University) for HCT-116 cells, Neil Bander (Weill Medical School Cornell University) for monoclonal antibody J591, Wei Dai (University of Oklahoma) for anti-BubR1 antibody, and Kuan-Teh Jeang (NIH) for anti-Mad2 antibody and Dr. Gregory Payne for critical reading of the article.

References

- Rajasekaran AK, Anilkumar G, Christiansen JJ. Is prostate-specific membrane antigen a multifunctional protein? *Am J Physiol Cell Physiol* 2005;288:C975–81.
- Ghosh A, Heston WD. Tumor target prostate specific membrane antigen (PSMA) and its regulation in prostate cancer. *J Cell Biochem* 2004;91:528–39.
- Wright GL, Jr., Grob BM, Haley C, et al. Upregulation of prostate-specific membrane antigen after androgen-deprivation therapy. *Urology* 1996;48:326–34.
- Cleveland DW, Mao Y, Sullivan KF. Centromeres and kinetochores: from epigenetics to mitotic checkpoint signaling. *Cell* 2003;112:407–21.
- Georgi AB, Stukenberg PT, Kirschner MW. Timing of events in mitosis. *Curr Biol* 2002;12:105–14.
- Fang G. Checkpoint protein BubR1 acts synergistically with Mad2 to inhibit anaphase-promoting complex. *Mol Biol Cell* 2002;13:755–66.
- Potapova TA, Daum JR, Pittman BD, et al. The reversibility of mitotic exit in vertebrate cells. *Nature* 2006;440:954–8.
- Piel M, Nordberg J, Euteneuer U, Bornens M. Centrosome-dependent exit of cytokinesis in animal cells. *Science* 2001;291:1550–3.
- Wakefield JG, Huang JY, Raff JW. Centrosomes have a role in regulating the destruction of cyclin B in early *Drosophila* embryos. *Curr Biol* 2000;10:1367–70.
- Kraft C, Herzog F, Gieffers C, et al. Mitotic regulation of the human anaphase-promoting complex by phosphorylation. *EMBO J* 2003;22:6598–609.
- Fraschini R, Formenti E, Lucchini G, Piatti S. Budding yeast Bub2 is localized at spindle pole bodies and activates the mitotic checkpoint via a different pathway from Mad2. *J Cell Biol* 1999;145:979–91.
- Howell BJ, Hoffman DB, Fang G, Murray AW, Salmon ED. Visualization of Mad2 dynamics at kinetochores, along spindle fibers, and at spindle poles in living cells. *J Cell Biol* 2000;150:1233–50.
- Jin DY, Spencer F, Jeang KT. Human T cell leukemia virus type 1 oncoprotein Tax targets the human mitotic checkpoint protein MAD1. *Cell* 1998;93:81–91.
- Pereira G, Manson C, Grindlay J, Schiebel E. Regulation of the Bfa1p-Bub2p complex at spindle pole bodies by the cell cycle phosphatase Cdc14p. *J Cell Biol* 2002;157:367–79.
- Bharadwaj R, Yu H. The spindle checkpoint, aneuploidy, and cancer. *Oncogene* 2004;23:2016–27.
- Musacchio A, Salmon ED. The spindle-assembly checkpoint in space and time. *Nat Rev Mol Cell Biol* 2007;8:379–93.
- Cahill DP, Lengauer C, Yu J, et al. Mutations of mitotic checkpoint genes in human cancers. *Nature* 1998;392:300–3.
- Grady WM. Genomic instability and colon cancer. *Cancer Metastasis Rev* 2004;23:11–27.
- Hernando E, Orlow I, Liberal V, Nohales G, Benzra R, Cordon-Cardo C. Molecular analyses of the mitotic checkpoint components hSMAD2, hBUB1 and hBUB3 in human cancer. *Int J Cancer* 2001;95:223–7.
- Iwanaga Y, Chi YH, Miyazato A, et al. Heterozygous deletion of mitotic arrest-deficient protein 1 (MAD1) increases the incidence of tumors in mice. *Cancer Res* 2007;67:160–6.
- Michel L, Diaz-Rodriguez E, Narayan G, Hernando E, Murty VV, Benzra R. Complete loss of the tumor suppressor MAD2 causes premature cyclin B degradation and mitotic failure in human somatic cells. *Proc Natl Acad Sci U S A* 2004;101:4459–64.
- Song MS, Song SJ, Ayad NG, et al. The tumour suppressor RASSF1A regulates mitosis by inhibiting the APC-Cdc20 complex. *Nat Cell Biol* 2004;6:129–37.
- Chang SS, Reuter VE, Heston WD, Bander NH, Grauer LS, Gaudin PB. Five different anti-prostate-specific membrane antigen (PSMA) antibodies confirm PSMA expression in tumor-associated neovasculature. *Cancer Res* 1999;59:3192–8.

24. Anilkumar G, Rajasekaran SA, Wang S, Hankinson O, Bander NH, Rajasekaran AK. Prostate-specific membrane antigen association with filamin A modulates its internalization and NAALADase activity. *Cancer Res* 2003;63:2645–8.
25. Christiansen JJ, Rajasekaran SA, Moy P, et al. Polarity of prostate specific membrane antigen, prostate stem cell antigen, and prostate specific antigen in prostate tissue and in a cultured epithelial cell line. *Prostate* 2003;55:9–19.
26. Christiansen JJ, Rajasekaran SA, Inge L, et al. *N*-glycosylation and microtubule integrity are involved in apical targeting of prostate-specific membrane antigen: implications for immunotherapy. *Mol Cancer Ther* 2005;4:704–14.
27. Rajasekaran SA, Anilkumar G, Oshima E, et al. A novel cytoplasmic tail MXXXL motif mediates the internalization of prostate-specific membrane antigen. *Mol Biol Cell* 2003;14:4835–45.
28. Liu H, Moy P, Kim S, et al. Monoclonal antibodies to the extracellular domain of prostate-specific membrane antigen also react with tumor vascular endothelium. *Cancer Res* 1997;57:3629–34.
29. Krishan A. Rapid flow cytofluorometric analysis of mammalian cell cycle by propidium iodide staining. *J Cell Biol* 1975;66:188–93.
30. Wu H, Lan Z, Li W, et al. p55CDC/hCDC20 is associated with BUBR1 and may be a downstream target of the spindle checkpoint kinase. *Oncogene* 2000;19:4557–62.
31. King RW, Deshaies RJ, Peters JM, Kirschner MW. How proteolysis drives the cell cycle. *Science* 1996;274:1652–9.
32. Peters JM. The anaphase promoting complex/cyclosome: a machine designed to destroy. *Nat Rev Mol Cell Biol* 2006;7:644–56.
33. Sudakin V, Ganoth D, Dahan A, et al. The cyclosome, a large complex containing cyclin-selective ubiquitin ligase activity, targets cyclins for destruction at the end of mitosis. *Mol Biol Cell* 1995;6:185–97.
34. Herzog F, Peters J. Large-scale purification of the vertebrate anaphase-promoting complex/cyclosome. In: Deshaies RJ, editor. *Methods in enzymology*. Academic Press; 2005. p. 175–95.
35. Tang Z, Yu H. Functional analysis of the spindle-checkpoint proteins using an *in vitro* ubiquitination assay. In: Schoenthal AH, editor. *Checkpoint controls and cancer*. Totowa (NJ): Humana Press; 2004. p. 227–42.
36. Yu H. Regulation of APC-Cdc20 by the spindle checkpoint. *Curr Opin Cell Biol* 2002;14:706–14.
37. Fodde R, Kuipers J, Rosenberg C, et al. Mutations in the APC tumour suppressor gene cause chromosomal instability. *Nat Cell Biol* 2001;3:433–8.
38. Rajagopalan H, Jallepalli PV, Rago C, et al. Inactivation of hCDC4 can cause chromosomal instability. *Nature* 2004;428:77–81.
39. Liu H, Rajasekaran AK, Moy P, et al. Constitutive and antibody-induced internalization of prostate-specific membrane antigen. *Cancer Res* 1998;58:4055–60.
40. Okamoto CT, McKinney J, Jeng YY. Clathrin in mitotic spindles. *Am J Physiol Cell Physiol* 2000;279:C369–74.
41. Royle SJ, Bright NA, Lagnado L. Clathrin is required for the function of the mitotic spindle. *Nature* 2005;434:1152–7.
42. Hobdy-Henderson KC, Hales CM, Lapierre LA, Cheney RE, Goldenring JR. Dynamics of the apical plasma membrane recycling system during cell division. *Traffic* 2003;4:681–93.
43. Reimann JD, Freed E, Hsu JY, Kramer ER, Peters JM, Jackson PK. Emi1 is a mitotic regulator that interacts with Cdc20 and inhibits the anaphase promoting complex. *Cell* 2001;105:645–55.
44. Liu B, Hong S, Tang Z, Yu H, Giam CZ. HTLV-I Tax directly binds the Cdc20-associated anaphase-promoting complex and activates it ahead of schedule. *Proc Natl Acad Sci U S A* 2005;102:63–8.
45. Casaletto JB, Nutt LK, Wu Q, et al. Inhibition of the anaphase-promoting complex by the Xnf7 ubiquitin ligase. *J Cell Biol* 2005;169:61–71.
46. Clute P, Pines J. Temporal and spatial control of cyclin B1 destruction in metaphase. *Nat Cell Biol* 1999;1:82–7.
47. Reddy SK, Rape M, Margansky WA, Kirschner MW. Ubiquitination by the anaphase-promoting complex drives spindle checkpoint inactivation. *Nature* 2007;446:921–5.
48. Stegmeier F, Rape M, Draviam VM, et al. Anaphase initiation is regulated by antagonistic ubiquitination and deubiquitination activities. *Nature* 2007;446:876–81.
49. Bander NH, Nanus DM, Milowsky MI, Kostakoglu L, Vallabhaajosula S, Goldsmith SJ. Targeted systemic therapy of prostate cancer with a monoclonal antibody to prostate-specific membrane antigen. *Semin Oncol* 2003;30:667–76.